




REGULAR ARTICLE

Influence of the Substrate Material on the Structural Properties
of Cadmium Telluride Films

A.V. Meriuts, G.S. Khrypunov, M.M. Kharchenko, A.I. Dobrozhan,
R.V. Zaitsev* , M.V. Kirichenko, K.O. Minakova, A.M. Drozdov

National Technical University "Kharkiv Polytechnic Institute", 61002 Kharkiv, Ukraine

(Received 10 April 2024; revised manuscript received 20 August 2024; published online 27 August 2024)

With the use of modernized industrial vacuum installations, a series of test samples of cadmium telluride films was produced by the method of thermal vacuum evaporation on glass substrates without a sublayer of transparent conductive oxide, with a sublayer of conductive oxide, and on molybdenum foil substrates to study the influence of the substrate material on the structural parameters of the test samples. The study of the structure was carried out by the method of X-ray diffractometric analysis, the parameters of the lattice, the sizes of the regions of coherent scattering and the texture coefficient of the film were calculated. Based on the results of research into the structural parameters of samples made on a glass substrate, the presence of a cubic phase of cadmium telluride was established. It is shown that when the temperature of the substrate increases, the texture of the samples increases and the presence of tensile stresses is observed, since the lattice period of the cubic phase is significantly higher than that of the tabular phase. For a sample obtained on a glass substrate with a layer of transparent conductive ITO oxide at a substrate temperature of 200 °C, the presence of two hexagonal phases H1 and H2 and a cubic phase C was established. The samples obtained on a molybdenum foil substrate contain almost entirely the cubic CdTe phase only in very thin sample no. 1 traces of the hexagonal phase are present. For the first thinnest sample, only one main diffraction peak of the cubic phase is observed, which can be explained by the fact that in the initial stages of the film growth, it grows as a highly textured cubic phase with the possible presence of some hexagonal phase. From the analysis of the obtained results, it can be noted that the samples obtained on the molybdenum substrate have a lattice parameter closest to the table data – 6.482-6.483 Å. The structural differences observed between the studied samples are due to the fact that they have a different preferred orientation, which is most likely due to a change in the sputtering speed.

Keywords: Cadmium Telluride, Structure, Lining, Grille, Texture.

DOI: [10.21272/jnep.16\(4\).04023](https://doi.org/10.21272/jnep.16(4).04023)

PACS numbers: 84.60. – h, 61.43.Bn

1. INTRODUCTION

Cadmium telluride (CdTe) has remained one of the most popular thin-film semiconductor materials for creating economical and efficient device structures, particularly thin-film solar cells for terrestrial applications [1, 2]. This is attributed to its optimal bandgap for photoelectric conversion under terrestrial conditions, high optical absorption coefficient enabling the use of thick absorber layers of a few micrometers [3], and the availability of material- and energy-efficient CdTe film deposition technologies [4]. The world leader in industrial production of the most efficient CdS/CdTe solar modules is the company First Solar (USA) [4, 5]. In 2020, the total electrical capacity of First Solar's manufactured solar modules reached 2.4 GW [6]. In recent years, there has been a growing number of studies focusing on the application of cadmium telluride in device structures for purposes other than solar cells. In particular, the rapid switching effect between high and low conductivity states in CdTe has been discovered and actively researched. This effect can be utilized to create memory devices based on cadmium telluride.

Additionally, there is potential for investigating the possibility of creating electronic device protection elements against electromagnetic pulses by exploiting the rapid switching effect in structures based on cadmium telluride. Commercial prospects have intensified scientific research in developing the physical and technical foundations of industrial technologies for obtaining device structures based on CdTe [7-11]. Since the operation principle of these device structures is based on kinetic charge carrier transport processes, and the crystalline structure of the thin film directly influences the charge carrier parameters [12-17], the study of the influence of substrate materials on the structural properties of thin cadmium telluride films is a relevant task in thin-film materials science.

The investigation focuses on the influence of the substrate material on which thin films of cadmium telluride (CdTe) are deposited on their structural properties.

2. CdTe BASED SAMPLES PREPARATION AND SAMPLES TESTING TECHNIQUE

* Correspondence e-mail: zaitsev@khpi.edu.ua



In the upgraded vacuum system UVN-74, layers of cadmium telluride (CdTe) were implemented and fabricated using the thermal vacuum evaporation method at various technological parameters of the substrate temperature ranging from 100 to 300 °C. The initial vacuum level in the vacuum chamber was maintained at 10^{-5} Pa. The thickness of the obtained samples and the deposition rate were monitored using optical methods after the deposition process. The deposition of CdTe layers took place on glass substrates without a transparent conductive oxide sublayer to investigate the thickness and deposition rate of the layers, and with a sublayer of conductive oxide to study the influence of the substrate material on the structural parameters of the test samples.

Additionally, the process of vacuum thermal evaporation was implemented in the VUP-5M vacuum system using a modernized vacuum chamber fixture. This modernization was necessitated by the limitations of the standard capabilities for implementing the vacuum evaporation process in this setup. Moreover, this vacuum chamber has a smaller volume, allowing for an accelerated process of obtaining basic functional layers of cadmium telluride, considering the preparatory processes for thermal deposition. To obtain thin semiconductor films of CdTe using the thermal vacuum deposition method, a fixture was developed and manufactured, including a resistive evaporator and a substrate heater, adapted to the design of the standard industrial vacuum system VUP-5M (Figure 1).

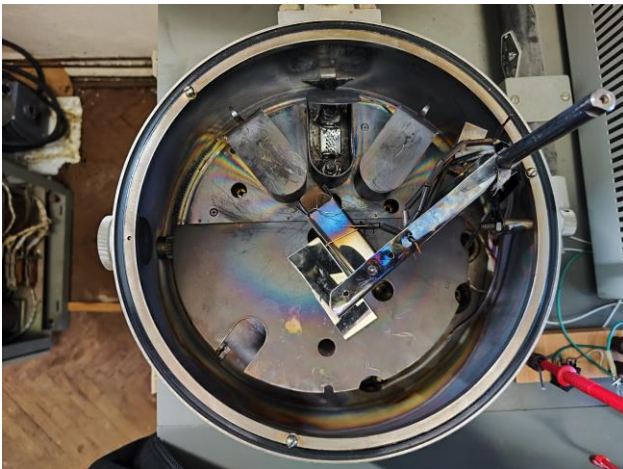


Fig. 1 – Photograph of the thermal vacuum deposition system in the VUP-5M vacuum system

Cadmium telluride layers were obtained at substrate temperatures $T_s = 350-400$ °C, defining this process as a low-temperature method for producing semiconductor layers. The initial vacuum level in the vacuum chamber of this setup was 10^{-4} Pa. Molybdenum foil substrates were used to obtain test samples of protective elements. The deposition time was controlled to monitor the formation of the cadmium telluride layer.

For the investigation of structural characteristics, a series of samples of the base layer were fabricated from CdTe films on conductive substrates, which could serve as one of the contacts in the device structure during its fabrication in a vertical configuration. Additionally, samples were fabricated on a dielectric substrate, which could be used as a base for the device structure

in a horizontal configuration. The samples were produced using the thermal evaporation method, and the structural analysis was conducted using X-ray diffractionometry on a D8 DISCOVER diffractometer (BRUKER) with θ - 2θ scanning in copper anode radiation.

3. STRUCTURAL PROPERTIES OF CADMIUM TELLURIDE FILMS

Figures 2, 3, and 4 depict the diffraction patterns of the CdTe film obtained on a glass substrate at substrate temperatures of 100, 200, and 300 °C, respectively. Tables 1, 2, and 3 present the results of the diffraction analysis (intensity I , integral intensity I_{int} , lattice parameter d , full width at half maximum FWHM). Calculations of lattice parameters, coherent scattering domain (CSD) sizes, and film texture coefficients are provided in Table 4.

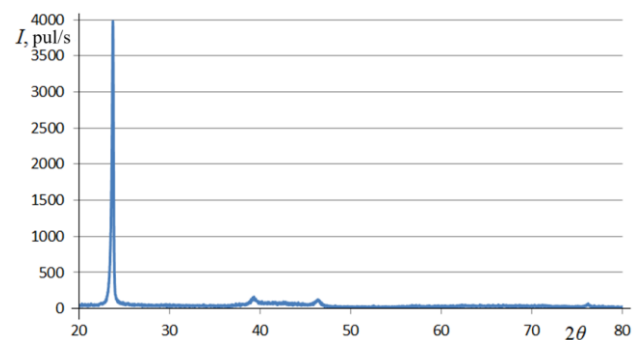


Fig. 2 – Diffraction pattern of the CdTe film obtained on a glass substrate at a substrate temperature of 100 °C

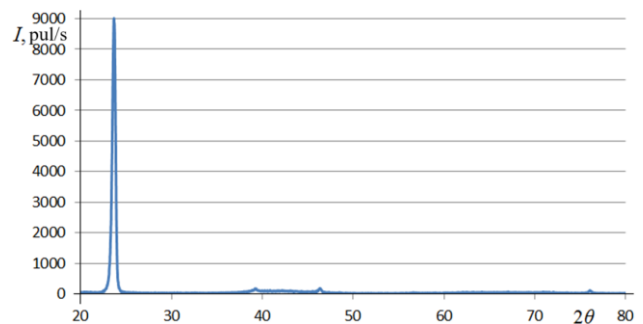


Fig. 3 – Diffraction pattern of the CdTe film obtained on a glass substrate at a substrate temperature of 200 °C

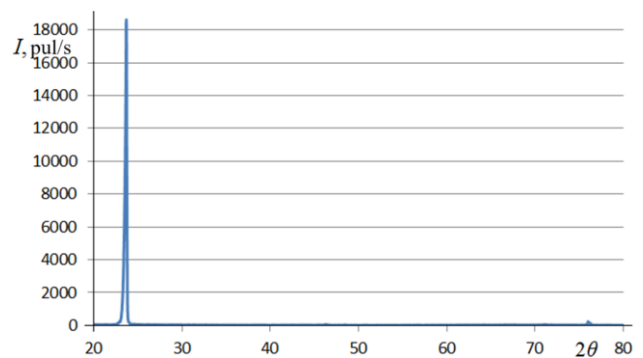


Fig. 4 – Diffraction pattern of the CdTe film obtained on a glass substrate at a substrate temperature of 300 °C

Table 1 – Results of the diffraction analysis of the CdTe film obtained on a glass substrate at a substrate temperature of 100 °C

CdTe	2θ, deg	I, pulse	d, Å	I _{int} , pulse	FWHM, deg
H1 (002)	23.70688	2715.06	3.74986	707.06	0.26487
H1 (110)	39.2007	42.33	2.29613	33.16	0.78327
galo	39.5-46				
C (311)	46.30546	40.16	1.95902	30.2	0.74778
H1 (006)	76.06612	17.22	1.25018	11.07	0.64201

As indicated by the results presented in Table 1, for this sample obtained on a glass substrate at a substrate temperature of 100 °C, only one phase can confidently be identified. This phase is denoted in the table as **H1**, and identified as the hexagonal phase of CdTe, which, according to the JSPDC-19-0193 table, has a P63mc (186) structure with tabulated lattice parameter values $a = 4.58 \text{ \AA}$, $c = 7.50 \text{ \AA}$.

On the diffraction pattern, there is also an observed peak at an angle of 46.305°, which may correspond to the cubic phase of CdTe, indicated in the table by the letter **c** and, according to the tables JSPDC-15-0770, 65-0440, 65-0880, 65-1081, 65-1082, 65-1085, 65-8395, has an F43m (216) structure with tabulated lattice parameter values of $a = 6.48\text{-}6.483 \text{ \AA}$. However, based on a single peak, it is not possible to definitively identify the presence of the phase; nevertheless, from the analysis of subsequent samples, it can be inferred that the cubic phase may indeed be present in this sample [18-21].

The halo between angles 39-46° indicates a low structural quality of the film, which is a consequence of the low substrate temperature.

Table 2 – Results of the diffraction analysis of the CdTe film obtained on a glass substrate at a substrate temperature of 200 °C

CdTe	2θ, deg	I, pulse	d, Å	I _{int} , pulse	FWHM, deg
H1 (002)	23.67294	5960.17	3.75516	2797.12	0.46904
H1 (110)	39.21402	34.34	2.29538	9.85	0.28687
galo	39.5-46				
C (311)	46.33094	69.52	1.958	30.33	0.44485
C (400)	56.6096	7.29	1.62446	6.6	0.90505
C (331)	62.28231	4.82	1.48943	3.68	0.76556
H1 (300)	71.03671	5.73	1.32582	4.83	0.84315
H1 (006)	76.04768	49.41	1.25044	21.62	0.43762

As indicated by the results presented in Table 2, for this sample obtained on a glass substrate at a substrate temperature of 200 °C, the presence of two phases – hexagonal and cubic – can confidently be identified. Peaks at angles 39 and 71 degrees with equal probability may belong to either the cubic or hexagonal phase, and unfortunately, they could not be distinguished. Additional investigations are needed to determine their specific attribution.

For the sample obtained on a glass substrate at a substrate temperature of 300 °C, it is likely that there is a higher proportion of the cubic phase. However, with an increase in substrate temperature, the first

peak shifts towards smaller angles. For the cubic phase, it should shift towards larger angles. Therefore, it cannot be completely ruled out that the hexagonal phase is present, and the possibility of its presence in this sample is still considered.

Table 3 – Results of the diffraction analysis of the CdTe film obtained on a glass substrate at a substrate temperature of 300 °C

CdTe	2θ, deg	I, pulse	d, Å	I _{int} , pulse	FWHM, deg
H1 (002)	23.68978	12102.8	3.75253	3454.4	0.29202
C (111)					
C (311)	46.2483	19.96	1.96131	10.54	0.52928
C (222)	48.4302	7.36	1.87792	3.02	0.3956
H1 (300)	71.11673	8.89	1.32453	5.01	0.56534
C (422)					
H1 (006)	76.01848	156.94	1.25084	44.65	0.28447
C (333)					

Table 4 summarizes the results of the calculation of lattice parameters, CSD sizes, and stresses for the phase **H1**, with paired multiple peaks and for the sample obtained at a substrate temperature of 300 °C, where multiple peaks can be attributed to the cubic phase.

Table 4 presents lattice parameters, CSD sizes, and stresses for the identified phases in CdTe films obtained on a glass substrate.

Table 4 – Lattice parameters, CSD sizes and stresses for the identified phases in CdTe films obtained on a glass substrate

H1: $a = 4.58 \text{ \AA}$, $c = 7.50 \text{ \AA}$							C: $a = 6.48\text{-}6.483 \text{ \AA}$		
T_{sb} , °C	c , Å	a , Å	L , nm		ϵ		G	G	a , Å
			min	max	min	max			
100	7.501	4.593	1.84	2.33	-0.0651	-0.2555	1.08		6.497
200	7.503	4.593	3.37	3.54	0.0087	0.0358	1.63	0.47	6.495
300	7.505	4.588	5.09	5.43	-0.0046	-0.0294	1.26		
Cubic phase 300 °C			4.54	4.68	-0.0065	-0.0295		1.33	6.493

To calculate the lattice parameters, the least squares method was employed. The function used to account for systematic errors in the measurement of the diffraction pattern was $F(\theta) = \cos^2(\theta)$.

As seen from the results presented in Table 4, the coherent scattering domain sizes increase with rising temperature. Regardless of the film's phase composition, the main phase **H1** exhibits texture in all samples. With the increase in temperature from 100 to 200 °C, the texturing of the hexagonal phase also increases (Table 4). The absolute value of stresses decreases by an order of magnitude as the substrate temperature rises from 100 to 200 °C, and the stresses change from negative to positive. Since the lattice parameters of the hexagonal phase remain practically unchanged, the change in the sign of stresses may indirectly confirm the presence of the cubic phase [22-25]. With further temperature increase from 200 to 300 °C, the sign of stresses changes again, now from positive to negative, which could be associated with a decrease in the content of the hexagonal phase. Additionally, the lattice period of the cubic phase is significantly higher

than the tabulated value, suggesting that this phase may be subject to substantial tensile stresses.

Figures 5, 6, and 7 show the diffraction patterns of the CdTe film obtained on a glass substrate with a layer of transparent conductive oxide ITO (composition of SnO₂ and In₂O₃ powders) at substrate temperatures of 100, 200, and 300 °C, respectively [26, 27]. The results of the diffraction pattern analysis are presented in Tables 5, 6, and 7. Calculations of lattice parameters, CSD sizes, and the texture coefficient of the film are provided in Table 8.

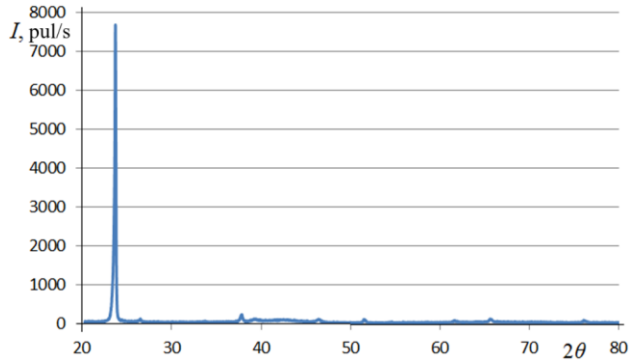


Fig. 5 – X-ray diffractogram of the CdTe film obtained on a glass substrate with a layer of transparent conductive oxide ITO at a substrate temperature of 100 °C

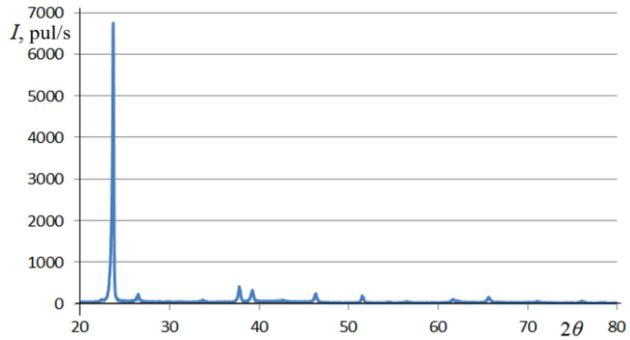


Fig. 6 – X-ray diffractogram of the CdTe film obtained on a glass substrate with a layer of transparent conductive oxide ITO at a substrate temperature of 200 °C

Table 5 – Results of the X-ray diffractogram analysis of the CdTe film obtained on a glass substrate with a layer of transparent conductive oxide ITO at a substrate temperature of 100 °C

	2θ, deg	I, pulse	d, Å	I_{int}, pulse	FWHM, deg
H1 (002)	23.71022	5241.6	3.74934	1144.7	0.2184
SnO ₂ (110)	26.47142	32.6	3.36418	12.32	0.3801
SnO ₂ (101)	33.6946	7.96	2.65768	4.95	0.6231
SnO ₂ (200)	37.77811	107.5	2.37926	36.8	0.3423
H1 (110) C (220)	39.27214	25.95	2.29212	14.59	0.5621
H1, H2 galo	42.496	24.30	2.12552	85.3	3.5097
H2 (201) C (311)	46.39332	36.86	1.95552	19.22	0.5216

SnO ₂ (211), In ₂ O ₃ (440)	51.47393	55.98	1.7738	19.09	0.3491
SnO ₂ (220)	54.5037	8.56	1.68214	3.5	0.4097
H2 (3 $\bar{1}$1)	61.58227	22.14	1.50467	9.41	0.4254
H2 (3 $\bar{1}$2)	65.5635	53.36	1.4226	19.77	0.3705
H1 (006) C (333)	76.07544	27.14	1.25005	11.29	0.4159
H2 (106)	78.34793	4.73	1.21938	2.47	0.5226

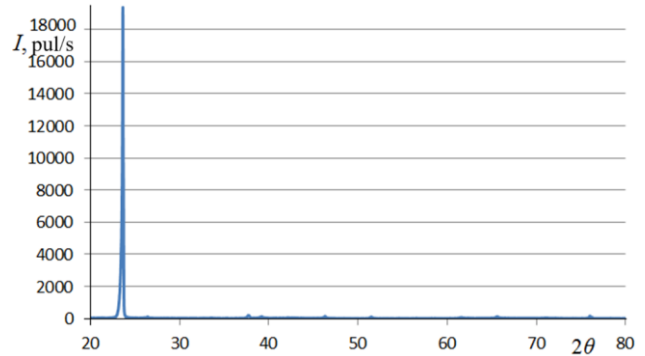


Fig. 7 – X-ray diffractogram of the CdTe film obtained on a glass substrate with a layer of transparent conductive oxide ITO at a substrate temperature of 300 °C

Table 6 – Results of the X-ray diffractogram analysis of the CdTe film obtained on a glass substrate with a layer of transparent conductive oxide ITO at a substrate temperature of 200 °C

	2θ, deg	I, pulse	d, Å	I_{int}, pulse	FWHM, deg
H1 (100)	22.3342	19.4	3.97713	4.45	0.2294
H1 (002)	23.68674	4332.6	3.753	1034.8	0.2294
SnO ₂ (110)	26.46571	93.7	3.36489	35.96	0.3836
SnO ₂ (101)	33.64761	23.1	2.66129	6.49	0.2808
SnO ₂ (200)	37.76602	215.9	2.38	77.2	0.3574
H1 (110) C (220)	39.21152	146.8	2.29553	57.2	0.3900
H2 (103)	41.831	5.03	2.157623	2.4	0.4684
H1 (103)	42.58	14.0	2.121392	13.9	0.9902
H2 (201) C (311)	46.26632	117.0	1.96059	42.6	0.3644
SnO ₂ (211), In ₂ O ₃ (440)	51.4848	95.3	1.77345	30	0.3115
SnO ₂ (220)	54.50231	10.7	1.68218	5.09	0.4778
C (400)	56.4814	14.0	1.62784	9.1	0.6498
H2 (3 $\bar{1}$1)	61.608	35.07	1.504102	23.6	0.6731
C (331) H1 (210)	62.222	11.9	1.490718	7.44	0.6267
H2 (3 $\bar{1}$2)	65.58257	80.2	1.42224	30.0	0.3737

H1 (300) C (422)	71.03127	20.4	1.32591	10.8	0.5348
H1 (006) C (333)	76.00232	25.7	1.25107	14.3	0.5483
H2 (106)	78.30629	7.6	1.21993	5.7	0.7492

As per the results presented in Table 5, for the sample obtained on a glass substrate with a layer of transparent conductive oxide ITO at a substrate temperature of 100 °C, two hexagonal phases can be confidently identified. The phase labeled as **H1** observed on glass substrates without a conductive layer, and the phase labeled as **H2** identified as the hexagonal phase of CdTe with the P63mc structure according to MDI JADE software #97-015-0941 with tabulated lattice parameters $a = 4.684 \text{ \AA}$, $c = 7.674 \text{ \AA}$.

Despite the presence of three peaks (220), (311), (333), which are closer to the cubic phase, and the first peak being closest to the cubic phase (111), there is no definitive reason to consider the presence of a cubic phase in this sample. No peak exclusively belongs to the cubic phase, and further investigations are needed to confirm its presence [28-32].

As per the results presented in Table 6, for the sample obtained on a glass substrate with a layer of transparent conductive oxide ITO at a substrate temperature of 200 °C, two hexagonal phases, **H1** and **H2** and a cubic phase **C** can be identified. This identification is possible because each of these phases has at least one reflection that exclusively belongs to that phase and does not overlap with others. Unfortunately, it is not possible to distinguish the reflections between phases **H1** and **C**.

Table 7 – Results of the X-ray diffractogram analysis of the CdTe film obtained on a glass substrate with a layer of transparent conductive oxide ITO at a substrate temperature of 300 °C

	2θ, deg	I, pulse	d, Å	I_{int}, pulse	FWHM, deg
H1 (002)	23.66102	13954.9	3.75702	2437.7	0.1761
SnO ₂ (110)	26.40661	25.62	3.37229	9.48	0.3706
SnO ₂ (101)	33.57044	11.49	2.66723	4.54	0.3959
SnO ₂ (200)	37.71313	109.95	2.38321	33.42	0.3039
H1 (110) C (220)	39.17154	49.81	2.29778	20.43	0.4101
H1, H2 galo	42.486	12.08	2.12596	26.07	2.1593
H2 (201) C (311)	46.26628	53.19	1.96059	21.02	0.3953
SnO ₂ (211), In ₂ O ₃ (440)	51.43654	46.56	1.775	15.77	0.3386
SnO ₂ (220)	54.4604	5.08	1.68337	2.12	0.4164
C (400)	56.60219	4.17	1.62465	1.79	0.4295
H2	61.52529	16.22	1.50593	7.44	0.4588

(3 11)					
H2 (3 12)	65.53529	51.52	1.42315	21.07	0.4044
H1 (300) C (422)	71.055	8.00	1.32553	7.5	0.9370
H2 (3 13)	71.919	2.44	1.311716	1.61	0.6583
H1 (006)	76.00239	113.23	1.25107	23.81	0.2104
H2 (106)	78.21225	5.56	1.22116	2.13	0.3751

With increasing substrate temperature, the most intense peak corresponding to the phase **H1** (002) shifts more towards smaller angles, and the orientation of grains of different phases changes. Some peaks disappear, while others emerge.

Table 8 presents the results of calculating lattice parameters, CSD sizes, and stresses for the **H1**, phase, for which a pair of multiple peaks were observed, as well as lattice parameters for the **H2** and **C** phases.

As evident from the results presented in Table 8, the CSD sizes increase with increasing temperature. Regardless of the film's phase composition, the main **H1** phase exhibits texture in samples obtained at all temperatures. The texture of the **H1** phase slightly decreases with the temperature increase from 100 to 200 °C, but significantly increases with further temperature elevation to 300 °C (Table 8). The absolute magnitude of stresses decreases by a factor of two with the temperature increase from 100 to 200 °C, and with further temperature rise, it changes from "+" to "-" and decreases by two orders of magnitude.

Table 8 – Lattice parameters, CSD sizes, and stresses for the phases identified in CdTe films obtained on glass substrates

H1							
$T_{sb}, \text{ }^\circ\text{C}$	$c, \text{ \AA}$	$a, \text{ \AA}$	$L, \text{ nm}$		ϵ		G
			min	max	min	max	
100	7.500	4.584	7.91	9.83	0.01141	0.06929	1.27
200	7.505	4.592	8.43	12.76	0.02528	0.12643	1.13
300	7.505	4.591	8.77	8.90	-0.0004	-0.004	1.58

H2			C	
$c, \text{ \AA}$	$a, \text{ \AA}$	G	$a, \text{ \AA}$	G
7.679	4.693	0.37	6.498	
7.677	4.685	0.55	6.492	0.26
7.666	4.659	0.71	6.491	0.44

Figures 8, 9, and 10 depict the diffraction patterns of the CdTe film obtained on a molybdenum foil substrate at a substrate temperature of 300 °C, while Tables 9, 10, and 11 present the results of the diffraction pattern analysis. The samples had different thicknesses: Sample #1 had a thickness of approximately 1-2 μm, Sample #2 had a thickness of about 3-4 μm, and Sample #3 had a thickness of around 4-5 μm.

Calculations of lattice parameters, CSD sizes, and texture coefficient for the CdTe film are presented in Table 12. Samples obtained on a molybdenum foil substrate contain the cubic phase of CdTe, and only in the very thin Sample #1, traces of the hexagonal phase may be present.

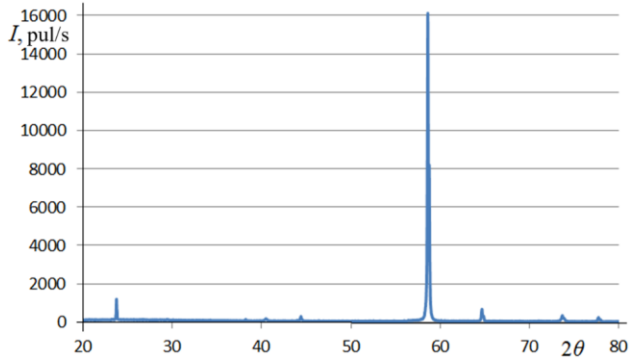


Fig. 8 – Diffraction pattern of the CdTe film (Sample #1, thickness ~ 1-2 μm) obtained on a molybdenum foil substrate

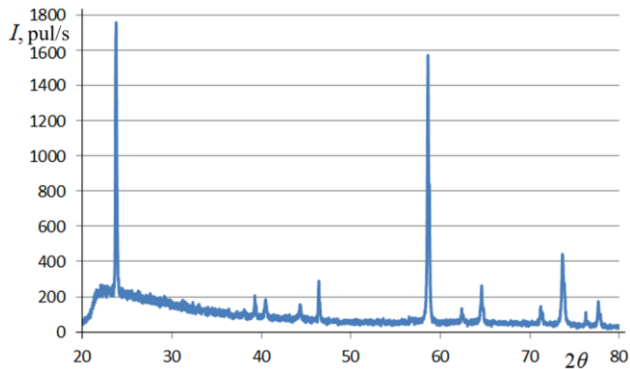


Fig. 9 – Diffraction pattern of the CdTe film (Sample #2, thickness ~ 3-4 μm) obtained on a molybdenum foil substrate

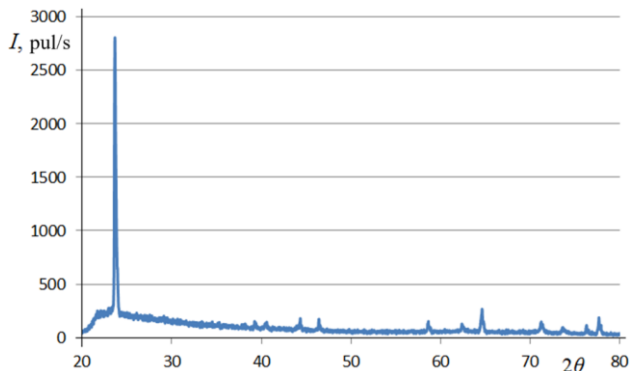


Fig. 10 – Diffraction pattern of the CdTe film (Sample #3, thickness ~ 4-5 μm) obtained on a molybdenum foil substrate

Table 9 – Results of the analysis of the diffraction pattern of the CdTe film (Sample #1, thickness ~ 1-2 μm) obtained on a molybdenum foil substrate

	2θ, deg	I, pulse	d, Å	I _{int} , pulse	FWHM, deg	a, Å
(111) CdTe, C	23.76582	55	3.74069	70.26	0.09128	6.479
(2 10) CdTe, H2	38.23092	41.79	2.35212	8.71	0.20843	
(110) Mo	40.45715	57.63	2.22768	21.28	0.36929	3.150
(200) Mo	58.6115	14630	1.57365	2159.53	0.14761	3.147

(211) Mo	73.64024	225.12	1.28525	65.6	0.29348	3.148
----------	----------	--------	---------	------	---------	-------

Table 12 presents the results of the lattice parameter, CSD sizes, and stresses calculations for the C phase of the CdTe film obtained on a molybdenum foil substrate. Regarding the first, thinnest sample, only one main diffraction peak of the cubic phase was observed. Therefore, it can be assumed that in the initial stages of film growth, it develops as a strongly textured cubic phase with the possible presence of some amount of hexagonal phase.

Table 10 – Results of the analysis of the diffraction pattern of the CdTe film (Sample #2, thickness ~ 3-4 μm) obtained on a molybdenum foil substrate

	2θ, deg	I, pulse	d, Å	I _{int} , pulse	FWHM, deg	a, Å
(111) CdTe	23.72026	1056	3.74778	194.18	0.18385	6.491345
(202) CdTe	39.25178	70.67	2.29326	11.6	0.164	6.486319
(110) Mo	40.43389	54.13	2.2289	13.25	0.24405	3.152141
(311) CdTe	46.401	159.5	1.95521	159.51	0.1342	6.484698
(400) CdTe	56.82571	15.22	1.62008	7.92	0.52009	6.480316
(200) Mo	58.6	1241	1.57393	244.84	0.19731	3.14786
(313) CdTe	62.37	45.13	1.48757	7.58	0.16585	6.484167
(242) CdTe	71.18824	50.8	1.32337	10.86	0.16135	6.483162
(211) Mo	73.64491	292	1.28518	77.62	0.26636	3.148035
(333) CdTe	76.23016	51.99	1.2479	9.06	0.17423	6.484279

Table 11 – Results of the analysis of the CdTe film diffraction pattern (sample №3, thickness ~ 4-5 μm) obtained on a molybdenum foil substrate

	2θ, deg	I, pulse	d, Å	I _{int} , pulse	FWHM, deg	a, Å
(111) CdTe	23.648	1122	3.75905	193.12	0.26168	6.511
(202) CdTe	39.24324	22.3	2.29374	6.8	0.20305	6.488
(110) Mo	40.48426	29.96	2.22625	11.9	0.39709	3.148
(311) CdTe	46.39861	44	1.95531	10.05	0.12693	6.485
(200) Mo	58.57904	55.38	1.57445	9.77	0.17638	3.149
(313) CdTe	62.37185	27.2	1.4875	6.97	0.15384	6.484
(242) CdTe	71.18728	36.8	1.32339	12.25	0.19627	6.483
(211) Mo	73.59378	27.68	1.28594	7.71	0.27837	3.150
(333) CdTe	76.2366	28.7	1.24781	10	0.18327	6.484

Table 12 – Lattice parameters, CSD sizes, and stresses for phases identified in CdTe films obtained on a molybdenum foil substrate

№	a , Å	L , nm		ε		G
		min	max	min	max	
1	6.479	–	–	–	–	
2	6.483	8.3	7.7	–0.0025	–0.026	0.85
3	6.482	5.8	4.9	–0.0083	–0.068	0.97

From the analysis of the obtained results, it can be noted that the lattice parameter for sample #1 is closest to the data from the table JSPDC-65-0890 ($a = 6.4775$ Å), for sample #2 corresponds to the data from table JSPDC-65-0440 ($a = 6.483$ Å), and the lattice parameter for sample #3 corresponds to the data from table JSPDC-65-0880 ($a = 6.482$ Å). Sample #2 has a more perfect structure, with larger CSD sizes and lower stresses, reflected in, on average, smaller integral widths of diffraction peaks for this sample. Structural differences between these samples are related to their different preferred orientation, which could have occurred due to variations in the sputtering rate.

4. CONCLUSIONS

Using upgraded industrial vacuum setups, a series of test samples of cadmium telluride films were fabricated through thermal vacuum evaporation on glass substrates without a transparent conductive oxide sublayer, with a conductive oxide sublayer, and on molybdenum foil substrates. This was done to investigate the influence of the substrate material on the structural parameters of the test samples.

The structural analysis was conducted through X-ray diffractometry, and the lattice parameters, coherent scattering domain sizes, and film texture coefficient were calculated.

The results of the structural parameters investigation for samples fabricated on glass substrates revealed the presence of a cubic phase of cadmium telluride. The content of this phase increases with the rise in the deposition temperature, reaching its maximum at a deposition temperature of 200 °C. The halo between angles 39–46° indicates low structural quality of the film, which is a consequence of the low substrate temperature.

It was demonstrated that with an increase in the substrate temperature, the texturing of the samples grows. The absolute value of stresses decreases by an order of magnitude as the substrate temperature increases from 100 to 200 °C, and the stresses change sign from "–" to "+". Since the lattice parameters of the hexagonal phase

remain practically unchanged during this process, the change in the sign of stresses can be indirect evidence of the appearance of the cubic phase. With further increase from 200 to 300 °C, the sign of stresses changes again, now from "+" to "–", which may be associated with a reduction in the content of the hexagonal phase. Additionally, the lattice period of the cubic phase is significantly higher than the tabulated value, indicating substantial tensile stresses on this phase.

For the sample obtained on a glass substrate with a layer of transparent conductive oxide ITO at a substrate temperature of 200 °C, the presence of two hexagonal phases, **H1** and **H2**, and a cubic phase **C**, was identified. Similar to samples obtained on purely glass substrates, it was found that the coherent scattering domain sizes increase with the temperature growth. Regardless of the film's phase composition, the main **H1** phase exhibits texture for samples obtained at all temperatures. With an increase in temperature from 100 to 200 °C, the texturing of the **H1** phase slightly decreases, but with further temperature increase to 300 °C, it significantly increases. The absolute value of stresses decreases by a factor of two as the substrate temperature increases from 100 to 200 °C, and with further temperature increase, the sign of stresses changes from "+" to "–" and decreases by two orders of magnitude.

Samples obtained on molybdenum foil substrates practically consist entirely of the cubic phase of CdTe, with only very thin sample No 1 showing traces of the hexagonal phase. For the thinnest sample (No 1), only one main diffraction peak of the cubic phase is observed, which can be explained by the fact that at the initial stages of film growth, it develops as a highly textured cubic phase with the possible presence of some amount of the hexagonal phase.

From the analysis of the obtained results, it can be noted that samples obtained on molybdenum substrates have lattice parameters closest to the tabulated data - 6.482-6.483 Å. The structural differences observed between the investigated samples are likely due to their different preferred orientations, possibly caused by changes in the deposition rate.

ACKNOWLEDGEMENTS

The work was carried out with the financial support of the National Research Foundation of Ukraine, scientific research and development project 2022.01/0014, "Development of an experimental sample of a film element to protect electronic equipment from pulses of electromagnetic radiation."

REFERENCES

1. A. Bosio, S. Pasini, N. Romeo, *Coatings* **10** No 4, 344 (2020).
2. A. Onno, C. Reich, S. Li, et. al., *Nat. Energy* **7**, 400 (2022).
3. S. Kumari, D. Suthar, Himanshu, M.S. Dhaka, *Comm. Inorgan. Chem.* **43** No 6, 429 (2023).
4. A. Bosio, G. Rosa, *Sol. Energy* **175**, 31 (2018).
5. M.A. Green, E.D. Dunlop, M. Yoshita, et. al., *Prog. Photovoltaic.* **32** No 1, 3 (2024).
6. FirstSolar Series 7 TR1 Datasheet. Available online: [https://www.firstsolar.com/-/media/First-Solar/Technical-](https://www.firstsolar.com/-/media/First-Solar/Technical-Documents/Series-7/Series-7-TR1-Datasheet.ashx)
7. I.M. Dharmadasa, A.E. Alam, A.A. Ojo, O.K. Echendu, *J. Mater. Sci.: Mater. Electron.* **30**, 20330 (2019).
8. G. Zeng, X. Liu, Y. Zhao, et. al., *Int. J. Photoenergy* **2019**, 3579587 (2019).
9. G. Kartopu, B.L. Williams, V. Zardetto, et. al., *Sol. Energy Mater. Sol. C.* **191**, 78 (2019).
10. A. Rasha, A. Deng, B. Li, et. al., *Prog. Photovoltaic.* **27** No 12, 1115 (2019).
11. O.A. Niasse, A. Diaw, M. Niane, et. al., *Am. J. Mater. Sci.*

- Eng.* 6 No 2, 43 (2018).
12. G.S. Khrypunov, V.R. Kopach, A.V. Meriuts, et. al., *Semiconductors* 45, 1505 (2011).
 13. S.Y. Nunoue, T. Hemmi, E. Kata, *J. Electrochem. Soc.* 137 No 4, 1248 (1990).
 14. D.W. Lane, K.D. Rogers, J.D. Painter, D.A. Wood, *Thin Solid Film* 361-362, 1 (2000).
 15. M.G. Khrypunov, R.V. Zaitsev, D.A. Kudii, A.L. Khrypunova, *J. Nano-Electron. Phys.* 10 No 1, 01016 (2018).
 16. B.E. McCandless, R.W. Birkmire, *26th IEEE Photovoltaic Special Conference*, 307 (1992).
 17. V.V. Eremenko, V.A. Sirenko, I.A. Gospodarev, et al., *J. Phys.: Conf. Ser.* 969 No 1, 012021 (2018).
 18. A. Romeo, E. Argegnani, *Energies* 14 No 6, 1684 (2021).
 19. B.K. Ghosh, I. Saad, K. Tze Kin Teo, S.K. Ghosh, *Optik* 206, 164278 (2020).
 20. M.V. Kirichenko, G.S. Khrypunov, M.G. Khrypunov, et. al., *IOP Conf. Ser.: Mater. Sci. Eng.* 459, 012009 (2018).
 21. V. Sirenko, I. Gospodarev, E. Syrkin, et al., *Low Temp. Phys.* 46 No 3, 232 (2020).
 22. D.W. Lane, *Sol. Energy Mater. Sol. C* 90 No 9, 1169 (2006).
 23. R.S. Hall, D. Lamb, S.J.C. Irvine, *Energy Sci. Eng.* 9 No 5, 606 (2021).
 24. G.S. Khrypunov, G.I. Kopach, R.V. Zaitsev, et. al., *J. Nano-Electron. Phys.* 9 No 2, 02008 (2017).
 25. I.B. Sapaev, S. Sadullaev, D. Babajanov, et. al., *E3S Web Conf.* 413, 04009 (2023).
 26. V.V. Eremenko, V.A. Sirenko, I.A. Gospodarev, et al., *Low Temp. Phys.* 42 No 2, 99 (2016).
 27. V.V. Eremenko, V.A. Sirenko, I.A. Gospodarev, et al., *Low Temp. Phys.* 43 No 11, 1657 (2017).
 28. M.V. Kirichenko, R.V. Zaitsev, A.I. Dobrozhan, et. al., *2017 IEEE International Young Scientists Forum on Applied Physics and Engineering*, 108 (2017).
 29. R.V. Zaitsev, G.S. Khrypunov, N.V. Veselova, et. al., *J. Nano-Electron. Phys.* 9 No 3, 03015 (2017).
 30. G.S. Khrypunov, V.O. Nikitin, O.L. Rezinkin, et. al., *J. Mater. Sci.: Mater. Electron.* 31 No 5, 3855 (2020).
 31. G.S. Khrypunov, O.V. Pirohov, T.A. Gorstka, et. al., *Semiconductors* 49 No 3, 394 (2015).
 32. I. Medved, A. Pyrohov, A. Romin, et. al., *Mater. Sci. Forum* 1038, 3 (2021).

Вплив матеріалу підкладки на структурні властивості плівок телуриду кадмію

A.V. Meriuts, G.S. Khrypunov, M.M. Харченко, A.I. Доброжан, P.V. Зайцев, M.V. Кириченко, K.O. Мінакова, A.M. Дроздов

Національний технічний університет «Харківський політехнічний інститут», 61002 Харків, Україна

З використанням модернізованих промислових вакуумних установок виготовлено серію дослідних зразків плівок телуриду кадмію методом термічного вакуумного напарювання на скляних підкладках без підшару з прозорого електропровідного оксиду, з підшаром з електропровідного оксиду та на підкладках з молібденової фольги дослідити вплив матеріалу підкладки на структурні параметри досліджуваних зразків. Дослідження структури проводили методом рентгенівської дифрактометрії, розраховували параметри ґратки, розміри областей когерентного розсіювання та текстурний коефіцієнт плівки. За результатами дослідження структурних параметрів зразків, виготовлених на скляній підкладці, встановлено наявність кубічної фази телуриду кадмію. Показано, що при підвищенні температури підкладки збільшується текстура зразків і спостерігається наявність розтягуючих напружень, оскільки період решітки кубічної фази значно більший, ніж пластинчастої. Для зразка, отриманого на скляній підкладці з шаром прозорого електропровідного оксиду ІТО при температурі підкладки 200 °С, встановлено наявність двох гексагональних фаз Н1 і Н2 та кубічної фази С. Зразки, отримані на підкладці з молібденової фольги, містять майже повністю кубічну фазу CdTe лише в дуже тонкому зразку № 1 присутні сліди гексагональної фази. Для першого найтоншого зразка спостерігається лише один головний дифракційний пік кубічної фази, що можна пояснити тим, що на початкових етапах росту плівка росте як високотекстурована кубічна фаза з можливою присутністю деяких гексагональних фаз. З аналізу отриманих результатів можна відзначити, що зразки, отримані на молібденовій підкладці, мають параметр ґратки, найбільш близький до табличних даних – 6,482-6,483 Å. Структурні відмінності, що спостерігаються між досліджуваними зразками, пов'язані з тим, що вони мають різну переважну орієнтацію, що, швидше за все, пов'язано зі зміною швидкості розпилення.

Ключові слова: Телурид кадмію, Структура, Облицювання, Решітка, Текстура.